









2-13

February 2013



TECH BRIEFS

NATIONAL AERONAUTICS AND SPACE ADMINISTRATION

-  **Technology Focus**
-  **Electronics/Computers**
-  **Software**
-  **Materials**
-  **Mechanics/Machinery**
-  **Manufacturing**
-  **Bio-Medical**
-  **Physical Sciences**
-  **Information Sciences**
-  **Books and Reports**

INTRODUCTION

Tech Briefs are short announcements of innovations originating from research and development activities of the National Aeronautics and Space Administration. They emphasize information considered likely to be transferable across industrial, regional, or disciplinary lines and are issued to encourage commercial application.

Additional Information on NASA Tech Briefs and TSPs

Additional information announced herein may be obtained from the NASA Technical Reports Server: <http://ntrs.nasa.gov>.

Please reference the control numbers appearing at the end of each Tech Brief. Information on NASA's Innovative Partnerships Program (IPP), its documents, and services is available on the World Wide Web at <http://www.ipp.nasa.gov>.

Innovative Partnerships Offices are located at NASA field centers to provide technology-transfer access to industrial users. Inquiries can be made by contacting NASA field centers listed below.

NASA Field Centers and Program Offices

Ames Research Center

David Morse
(650) 604-4724
david.r.morse@nasa.gov

Dryden Flight Research Center

Ron Young
(661) 276-3741
ronald.m.young@nasa.gov

Glenn Research Center

Kimberly A. Dalgleish-Miller
(216) 433-8047
kimberly.a.dalgleish@nasa.gov

Goddard Space Flight Center

Nona Cheeks
(301) 286-5810
nona.k.cheeks@nasa.gov

Jet Propulsion Laboratory

Dan Broderick
(818) 354-1314
daniel.f.broderick@jpl.nasa.gov

Johnson Space Center

John E. James
(281) 483-3809
john.e.james@nasa.gov

Kennedy Space Center

David R. Makufka
(321) 867-6227
david.r.makufka@nasa.gov

Langley Research Center

Michelle Ferebee
(757) 864-5617
michelle.t.ferebee@nasa.gov

Marshall Space Flight Center

Terry L. Taylor
(256) 544-5916
terry.taylor@nasa.gov

Stennis Space Center

Ramona Travis
(228) 688-3832
ramona.e.travis@ssc.nasa.gov

NASA Headquarters

Daniel Lockney,
Technology Transfer Program Executive
(202) 358-2037
daniel.p.lockney@nasa.gov

Small Business Innovation Research (SBIR) & Small Business Technology Transfer (STTR) Programs

Rich Leshner, Program Executive
(202) 358-4920
rleshner@nasa.gov



TECH BRIEFS

NATIONAL AERONAUTICS AND SPACE ADMINISTRATION



5 Technology Focus: Test & Measurement

- 5 Measurements of Ultra-Stable Oscillator (USO) Allan Deviations in Space
- 5 Gaseous Nitrogen Orifice Mass Flow Calculator
- 5 Validation of Proposed Metrics for Two-Body Abrasion Scratch Test Analysis Standards
- 6 Rover Low Gain Antenna Qualification for Deep Space Thermal Environments
- 6 Automated, Ultra-Sterile Solid Sample Handling and Analysis on a Chip
- 7 Measuring and Estimating Normalized Contrast in Infrared Flash Thermography
- 8 Spectrally and Radiometrically Stable, Wideband, Onboard Calibration Source



9 Manufacturing & Prototyping

- 9 High-Reliability Waveguide Vacuum/Pressure Window
- 9 Methods of Fabricating Scintillators With Radioisotopes for Beta Battery Applications
- 10 Magnetic Shield for Adiabatic Demagnetization Refrigerators (ADR)



11 Electronics/Computers

- 11 CMOS-Compatible SOI MESFETS for Radiation-Hardened DC-to-DC Converters
- 11 Silicon Heat Pipe Array
- 12 Adaptive Phase Delay Generator



13 Materials & Coatings

- 13 High-Temperature, Lightweight, Self-Healing Ceramic Composites for Aircraft Engine Applications
- 13 Treatment to Control Adhesion of Silicone-Based Elastomers
- 14 High-Temperature Adhesives for Thermally Stable Aero-Assist Technologies



15 Mechanics/Machinery

- 15 Rockballer Sample Acquisition Tool
- 16 Rock Gripper for Sampling, Mobility, Anchoring, and Manipulation



17 Physical Sciences

- 17 Advanced Magnetic Materials Methods and Numerical Models for Fluidization in Microgravity and Hypogravity
- 17 Data Transfer for Multiple Sensor Networks Over a Broad Temperature Range
- 18 Using Combustion Synthesis to Reinforce Berms and Other Regolith Structures
- 18 Visible-Infrared Hyperspectral Image Projector
- 19 Three-Axis Attitude Estimation With a High-Bandwidth Angular Rate Sensor



21 Software

- 21 Change_Detection.m
- 21 AGATE: Adversarial Game Analysis for Tactical Evaluation
- 21 Ionospheric Simulation System for Satellite Observations and Global Assimilative Modeling Experiments (ISOGAME)
- 22 An Extensible, User-Modifiable Framework for Planning Activities
- 22 Mission Operations Center (MOC) - Precipitation Processing System (PPS) Interface Software System (MPISS)



23 Information Technology

- 23 Automated 3D Damaged Cavity Model Builder for Lower Surface Acreage Tile on Orbiter
- 23 Mixed Linear/Square-Root Encoded Single-Slope Ramp Provides Low-Noise ADC With High Linearity for Focal Plane Arrays
- 24 RUSHMAPS: Real-time Uploadable Spherical Harmonic Moment Analysis for Particle Spectrometers
- 25 Powered Descent Guidance With General Thrust-Pointing Constraints
- 25 X-Ray Detection and Processing Models for Spacecraft Navigation and Timing



27 Bio-Medical

- 27 Extreme Ionizing-Radiation-Resistant Bacterium

This document was prepared under the sponsorship of the National Aeronautics and Space Administration. Neither the United States Government nor any person acting on behalf of the United States Government assumes any liability resulting from the use of the information contained in this document, or warrants that such use will be free from privately owned rights.



▶ Measurements of Ultra-Stable Oscillator (USO) Allan Deviations in Space

NASA's Jet Propulsion Laboratory, Pasadena, California

Researchers have used data from the GRAIL mission to the Moon to make the first in-flight verification of ultra-stable oscillators (USOs) with Allan deviation below 10^{-13} for 1-to-100-second averaging times. USOs are flown in space to provide stable timing and/or navigation signals for a variety of different science and programmatic missions.

The Gravity Recovery and Interior Laboratory (GRAIL) mission is flying twin spacecraft, each with its own USO and with a Ka-band crosslink used to

measure range fluctuations. Data from this crosslink can be combined in such a way as to give the relative time offsets of the two spacecrafts' USOs and to calculate the Allan deviation to describe the USOs' combined performance while orbiting the Moon. Researchers find the first direct in-space Allan deviations below 10^{-13} for 1-to-100-second averaging times comparable to pre-launch data, and better than measurements from ground tracking of an X-band carrier coherent with the USO. Fluctuations in

Earth's atmosphere limit measurement performance in direct-to-Earth links. In-flight USO performance verification was also performed for GRAIL's parent mission, the Gravity Recovery and Climate Experiment (GRACE), using both K-band and Ka-band crosslinks.

This work was done by Daphna G. Enzer, William M. Klipstein, Rabi T. Wang, and Charles E. Dunn of Caltech for NASA's Jet Propulsion Laboratory. Further information is contained in a TSP (see page 1). NPO-48705

▶ Gaseous Nitrogen Orifice Mass Flow Calculator

Lyndon B. Johnson Space Center, Houston, Texas

The Gaseous Nitrogen (GN2) Orifice Mass Flow Calculator was used to determine Space Shuttle Orbiter Water Spray Boiler (WSB) GN2 high-pressure tank source depletion rates for various leak scenarios, and the ability of the GN2 consumables to support cooling of Auxiliary Power Unit (APU) lubrication during entry. The data was used to support flight rationale concerning loss of an orbiter APU/hydraulic system and mission work-arounds.

The GN2 mass flow-rate calculator standardizes a method for rapid assessment of GN2 mass flow through various orifice sizes for various discharge coefficients, delta pressures, and temperatures. The calculator utilizes a 0.9-lb (0.4 kg) GN2 source regulated to 40 psia (≈ 276 kPa). These parameters correspond to the Space Shuttle WSB GN2 Source and Water Tank Bellows, but can be changed in the spreadsheet to accommodate any system parameters. The cal-

culator can be used to analyze a leak source, leak rate, gas consumables depletion time, and puncture diameter that simulates the measured GN2 system pressure drop.

The software is programmed into a Microsoft Excel Solver spreadsheet.

This work was done by Charles Rittrivi of The Boeing Company for Johnson Space Center. For further information, contact the JSC Innovation Partnerships Office at (281) 483-3809. MSC-24873-1

▶ Validation of Proposed Metrics for Two-Body Abrasion Scratch Test Analysis Standards

In principle, any scratch can be analyzed by this method.

John H. Glenn Research Center, Cleveland, Ohio

Abrasion of mechanical components and fabrics by soil on Earth is typically minimized by the effects of atmosphere and water. Potentially abrasive particles lose sharp and pointed geometrical features through erosion. In environments where such erosion does not exist, such as the vacuum of the Moon, particles retain sharp geometries associated with fracturing of their parent particles by

micrometeorite impacts. The relationship between hardness of the abrasive and that of the material being abraded is well understood, such that the abrasive ability of a material can be estimated as a function of the ratio of the hardness of the two interacting materials. Knowing the abrasive nature of an environment (abrasive)/construction material is crucial to designing durable equipment for

use in such surroundings.

The objective of this work was to evaluate a set of standardized metrics proposed for characterizing a surface that has been scratched from a two-body abrasion test. This is achieved by defining a new abrasion region termed "Zone of Interaction" (ZOI). The ZOI describes the full surface profile of all peaks and valleys, rather than just measuring a scratch width. The ZOI

has been found to be at least twice the size of a standard width measurement; in some cases, considerably greater, indicating that at least half of the disturbed surface area would be neglected without this insight. The ZOI is used to calculate a more robust data set of volume measurements that can be used to computationally reconstruct a resultant profile for detailed analysis. Documenting additional changes to various surface roughness parameters also allows key material attributes of importance to ultimate design applications to be quantified, such as depth of penetration and final abraded surface roughness. Furthermore, by investigating the use of custom scratch tips for specific needs, the usefulness of having an abrasion metric that can measure the displaced volume in this stan-

dardized manner, and not just by scratch width alone, is reinforced. This benefit is made apparent when a tip creates an intricate contour having multiple peaks and valleys within a single scratch.

The current innovation consists of a software-driven method of quantitatively evaluating a scratch profile. The profile consists of measuring the topographical features of a scratch along the length of the scratch instead of the width at one location. The digitized profile data is then fed into software code, which evaluates enough metrics of the scratch to reproduce the scratch from the evaluated metrics.

There are three key differences between the current art and this innovation. First, scratch width does not quantify how far from the center of the scratch damage oc-

curs (ZOI). Second, scratch width does not discern between material displacement and material removal from the scratch. Finally, several scratches may have the same width but different zones of interactions, different displacements, and different material removals. The current innovation allows quantitative assessment of all three.

This work was done by Kenneth W. Street, Jr. of Glenn Research Center; Ryan L. Kobrick of MIT, and David M. Klaus of the University of Colorado at Boulder. Further information is contained in a TSP (see page 1).

Inquiries concerning rights for the commercial use of this invention should be addressed to NASA Glenn Research Center, Innovative Partnerships Office, Attn: Steven Fedor, Mail Stop 4-8, 21000 Brookpark Road, Cleveland, Ohio 44135. Refer to LEW-18780-1.

Rover Low Gain Antenna Qualification for Deep Space Thermal Environments

NASA's Jet Propulsion Laboratory, Pasadena, California

A method to qualify the Rover Low Gain Antenna (RLGA) for use during the Mars Science Laboratory (MSL) mission has been devised. The RLGA antenna must survive all ground operations, plus the nominal 670 Martian sol mission that includes the summer and winter seasons of the Mars thermal environment. This qualification effort was performed to verify that the RLGA design, its bonding, and packaging processes are adequate.

The qualification test was designed to demonstrate a survival life of three times more than all expected ground testing, plus a nominal 670 Martian sol missions. Baseline RF tests and a visual inspection

were performed on the RLGA hardware before the start of the qualification test. Functional intermittent RF tests were performed during thermal chamber breaks over the course of the complete qualification test. For the return loss measurements, the RLGA antenna was moved to a test area. A vector network analyzer was calibrated over the operational frequency range of the antenna. For the RLGA, a simple return loss measurement was performed.

A total of 2,010 (3×670 or 3 times mission thermal cycles) thermal cycles was performed. Visual inspection of the RLGA hardware did not show any anomalies due to the thermal cycling.

The return loss measurement results of the RLGA antenna after the PQV (Package Qualification and Verification) test did not show any anomalies. The antenna pattern data taken before and after the PQV test at the uplink and downlink frequencies were unchanged. Therefore, the developed design of RLGA is qualified for a long-duration MSL mission.

This work was done by Rajeshuni Ramesham, Luis R. Amaro, Paula R. Brown, and Robert Usiskin of Caltech; and Jack L. Prater of Polytechnic High School for NASA's Jet Propulsion Laboratory. Further information is contained in a TSP (see page 1). NPO-48500

Automated, Ultra-Sterile Solid Sample Handling and Analysis on a Chip

This technique could be used in the pharmaceutical industry for the automated manipulation of small amounts of powdered drugs.

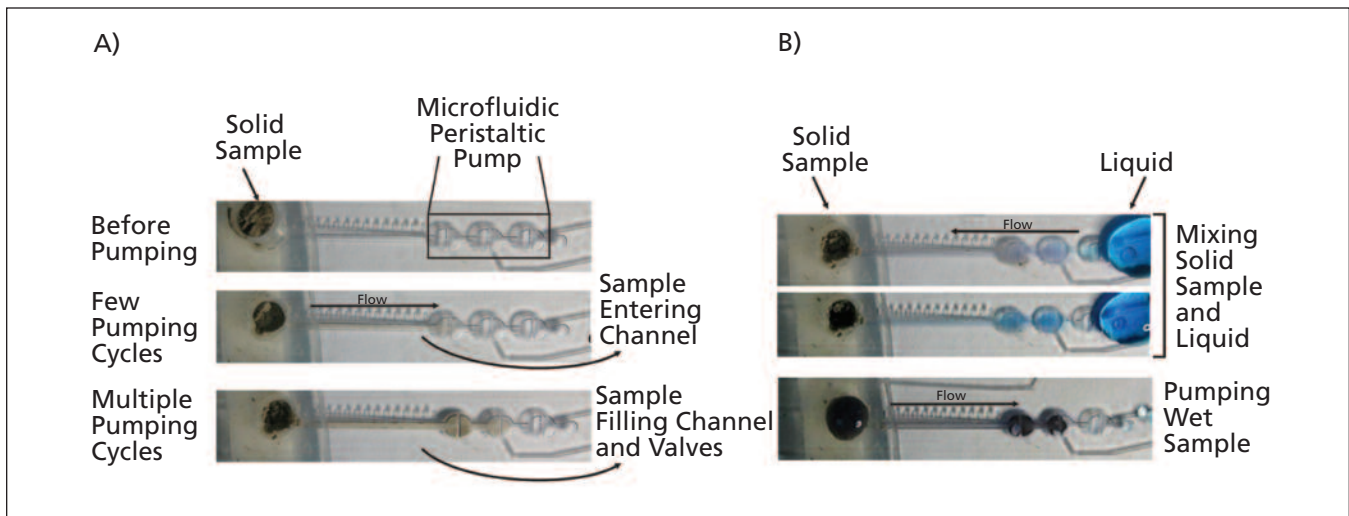
NASA's Jet Propulsion Laboratory, Pasadena, California

There are no existing ultra-sterile lab-on-a-chip systems that can accept solid samples and perform complete chemical analyses without human intervention. The proposed solution is to demonstrate completely automated lab-on-a-chip manipulation of powdered

solid samples, followed by on-chip liquid extraction and chemical analysis.

This technology utilizes a newly invented glass micro-device for solid manipulation, which mates with existing lab-on-a-chip instrumentation. Devices are fabricated in a Class 10 cleanroom at the

JPL MicroDevices Lab, and are plasma-cleaned before and after assembly. Solid samples enter the device through a drilled hole in the top. Existing micro-pumping technology is used to transfer milligrams of powdered sample into an extraction chamber where it is mixed with liquids to



(A) Manipulation of a **Solid Sample On-Chip**, and (B) mixing of fluid and solid sample on-chip. Each photograph is approximately 4x1 cm in size.

extract organic material. Subsequent chemical analysis is performed using portable microchip capillary electrophoresis systems (CE). These instruments have been used for ultra-highly sensitive (parts-per-trillion, ppt) analysis of organic compounds including amines, amino acids, aldehydes, ketones, carboxylic acids, and thiols. Fully autonomous amino acid analyses in liquids were demonstrated; however, to date there have been no reports of completely automated analysis of solid samples on chip.

This approach utilizes an existing portable instrument that houses optics, high-voltage power supplies, and sole-

noids for fully autonomous microfluidic sample processing and CE analysis with laser-induced fluorescence (LIF) detection. Furthermore, the entire system can be sterilized and placed in a cleanroom environment for analyzing samples returned from extraterrestrial targets, if desired.

This is an entirely new capability never demonstrated before. The ability to manipulate solid samples, coupled with lab-on-a-chip analysis technology, will enable ultraclean and ultrasensitive end-to-end analysis of samples that is orders of magnitude more sensitive than the ppb goal given in the Science Instruments, Obser-

vatories, and Sensor Systems Roadmap. This technology has potential applications for highly sensitive analyses of organic compounds elsewhere in the solar system, including Mars, Europa, Titan, and small bodies. It will also enable contamination-free analysis of returned samples. Finally, this could also be employed for a wide range of terrestrial applications including environmental, biomedical, or forensic analyses.

This work was done by Maria F. Mora, Amanda M. Stockton, and Peter A. Willis of Caltech for NASA's Jet Propulsion Laboratory. Further information is contained in a TSP (see page 1). NPO-48603

Measuring and Estimating Normalized Contrast in Infrared Flash Thermography

Combining temperature contrast analysis with pixel intensity contrast analysis yields better results in characterizing void-like anomalies.

Lyndon B. Johnson Space Center, Houston, Texas

Infrared flash thermography (IRFT) is used to detect void-like flaws in a test object. The IRFT technique involves heating up the part surface using a flash of flash lamps. The post-flash evolution of the part surface temperature is sensed by an IR camera in terms of pixel intensity of image pixels. The IR technique involves recording of the IR video image data and analysis of the data using the normalized pixel intensity and temperature contrast analysis method for characterization of void-like flaws for depth and width.

This work introduces a new definition of the normalized IR pixel intensity con-

trast and normalized surface temperature contrast. A procedure is provided to compute the pixel intensity contrast from the camera pixel intensity evolution data. The pixel intensity contrast and the corresponding surface temperature contrast differ but are related. This work provides a method to estimate the temperature evolution and the normalized temperature contrast from the measured pixel intensity evolution data and some additional measurements during data acquisition.

Thermal simulation software, such as Thermo-Calc, provides simulation of surface temperature evolution on void-

like flaws. A comparison of the experimentally estimated temperature contrast and simulation estimated temperature contrast is required to validate the simulation model and its input parameters. Conversely, if the simulation temperature contrast data is available, then a method provided here can be used to estimate the pixel intensity and the pixel intensity contrast based on known values of parameters of the data acquisition setup.

The normalized pixel intensity contrast and the normalized temperature contrast differ for objects with emissivity other than 1. Therefore, for better con-

trast analysis the two quantities should not be treated as the same. To compare the simulation temperature contrast with the measured pixel contrast, it is necessary to estimate the reflection temperature evolution. It is also necessary to estimate the incident heat flux. Ideally, the simulation should model the compound heat source flux evolution, which also includes the post-flash thermal afterglow. The effect of reflection temperature in the pixel intensity also should be accounted for to seek a better estimation of the temperature contrast evolution from the pixel intensity evolution data.

Using formulas given here, the reflection temperature evolution and the

temperature contrast evolution can be estimated from the IRFT data. An emissivity factor, defined here, relates the temperature contrast to the pixel intensity contrast.

Reflection temperature evolution can be used to model the afterglow flux of the flash source in the simulation to estimate the temperature contrast evolutions and the pixel intensity contrast evolution on simulated voids.

An emissivity estimation technique was developed using the IR camera. If the IR camera is programmed with the reflection temperature formulas derived here, the camera can provide the object surface temperature directly even during the IRFT data acquisition. The IR

camera can be programmed to estimate the object emissivity in real time using the technique provided here. Due to improvement in the contrast analysis, including the modeling of source in thermal simulation, void-like anomalies are characterized more precisely.

This work was done by Ajay M. Koshti of Johnson Space Center. Further information is contained in a TSP (see page 1).

This invention is owned by NASA, and a patent application has been filed. Inquiries concerning nonexclusive or exclusive license for its commercial development should be addressed to the Patent Counsel, Johnson Space Center, (281) 483-1003. Refer to MSC-24506-1.

Spectrally and Radiometrically Stable, Wideband, Onboard Calibration Source

NASA's Jet Propulsion Laboratory, Pasadena, California

The Onboard Calibration (OBC) source incorporates a medical/scientific-grade halogen source with a precisely designed fiber coupling system, and a fiber-based intensity-monitoring feedback loop that results in radiometric and spectral stabilities to within <0.3 percent over a 15-hour period. The airborne imaging spectrometer systems de-

veloped at the Jet Propulsion Laboratory incorporate OBC sources to provide auxiliary in-use system calibration data. The use of the OBC source will provide a significant increase in the quantitative accuracy, reliability, and resulting utility of the spectral data collected from current and future imaging spectrometer instruments.

This work was done by James B. Coles, Brandon S. Richardson, Michael L. Eastwood, Charles M. Sarture, Gregory R. Quetin, Michael D. Porter, Robert O. Green, Scott H. Nolte, Marco A. Hernandez, and Linley A. Kroll of Caltech for NASA's Jet Propulsion Laboratory. For more information, contact iaoffice@jpl.nasa.gov. NPO-47697



High-Reliability Waveguide Vacuum/Pressure Window

This design is suitable for commercial, military, and space applications requiring a helium-leak-tight vacuum pressure window.

NASA's Jet Propulsion Laboratory, Pasadena, California

The NASA Deep Space Network (DSN) uses commercial waveguide windows on the output waveguide of Ka-band (32 GHz) low-noise amplifiers. Mechanical failure of these windows resulted in an unacceptable loss in tracking time.

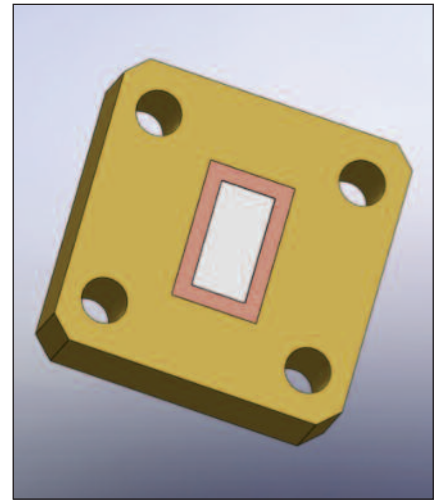
To address this issue, a new Ka-band WR-28 waveguide window has been designed, fabricated, and tested. The window uses a slab of low-loss, low-dielectric constant foam that is bonded into a ½-wave-thick waveguide/flange. The foam is a commercially available, rigid, closed-cell polymethacrylimide. It has excellent electrical properties with a dielectric constant of 1.04, and a loss tangent of 0.01. It is relatively strong with a tensile strength of 1 MPa. The material is virtually impermeable to helium. The finished window exhibits a leak rate of less than 3×10^{-3} cm³/s with helium. The material is also chemically resistant and can be cleaned with acetone.

The window is constructed by fabricating a window body by brazing a short length of WR-28 copper waveguide into a standard rectangular flange, and machining the resulting part to a thickness of 4.6 mm. The foam is machined to a

rectangular shape with a dimension of 7.06×3.53 mm. The foam is bonded into the body with a two-part epoxy. After curing, the excess glue and foam are knife-trimmed by hand. The finished window has a loss of less than 0.08 dB (2%) and a return loss of greater than 25 dB at 32 GHz. This meets the requirements for the DSN application. The window is usable for most applications over the entire 26-to-40-GHz waveguide band. The window return loss can be tuned to a required frequency by varying the thickness of the window slightly.

Most standard waveguide windows use a thin membrane of material bonded into a recess in a waveguide flange, or sandwiched between two flanges with a polymer seal. Designs using the recessed window are prone to mechanical failure over time due to constraints on the dimensions of the recess that allow the bond to fail. Designs using the sandwich method are often permeable to helium, which prohibits the use of helium leak detection.

At the time of this reporting, 40 windows have been produced. Twelve are in operation with a combined operating time of over 30,000 hours without a failure.



A solid model of the completed Waveguide Window assembly.

This work was done by Michael J. Britcliffe, Theodore R. Hanson, Ezra M. Long, and Steven Montanez of Caltech for NASA's Jet Propulsion Laboratory. Further information is contained in a TSP (see page 1). NPO-48372

Methods of Fabricating Scintillators With Radioisotopes for Beta Battery Applications

Applications for these power sources are implantable medical devices, power supplies for remote monitoring, and "trickle chargers" for consumer applications.

John H. Glenn Research Center, Cleveland, Ohio

Technology has been developed for a class of self-contained, long-duration power sources called beta batteries, which harvest the energy contained in the radioactive emissions from beta decay isotopes. The new battery is a significant improvement over the conventional phosphor/solar cell concept for converting this energy in three ways. First, the thin phosphor is replaced with a thick scintillator that is transparent to

its own emissions. By using a scintillator sufficiently thick to completely stop all the beta particles, efficiency is greatly improved. Second, since the energy of the beta particles is absorbed in the scintillator, the semiconductor photodetector is shielded from radiation damage that presently limits the performance and lifetime of traditional phosphor converters. Finally, instead of a thin film of beta-emitting material, the isotopes

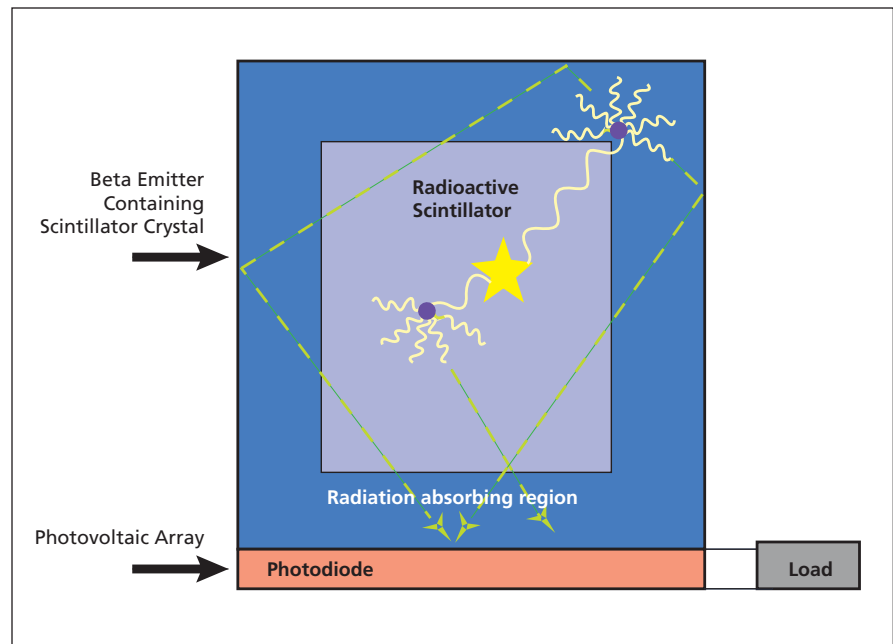
are incorporated into the entire volume of the thick scintillator crystal allowing more activity to be included in the converter without self-absorption.

There is no chemical difference between radioactive and stable strontium beta emitters such as Sr-90, so the beta emitter can be uniformly distributed throughout a strontium based scintillator crystal. When beta emitter material is applied as a foil or thin film to the sur-

face of a solar cell or even to the surface of a scintillator, much of the radiation escapes due to the geometry, and some is absorbed within the layer itself, leading to inefficient harvesting of the energy. In contrast, if the emitting atoms are incorporated within the scintillator, the geometry allows for the capture and efficient conversion of the energy of particles emitted in any direction. Any gamma rays associated with secondary decays or Bremsstrahlung photons may also be absorbed within the scintillator, and converted to lower energy photons, which will in turn be captured by the photocell or photodiode.

Some energy will be lost in this two-stage conversion process (high-energy particle to low-energy photons to electric current). The geometric advantage partially offsets this as well, since the absorption depth of high-energy beta radiation is much larger than the depth of a p-n junction. Thus, in a p-n junction device, much of the radiation is absorbed far away from the junction, and the electron-hole pairs are not all effectively collected. In contrast, with a transparent scintillator the radiation can be converted to light in a larger volume, and all of the light can be collected in the active region of the photodiode.

Finally, the new device is more practical because it can be used at much higher power levels without unduly shortening its lifetime. While the crystal structure of scintillators is also subject to radiation



The **Scintillator-Based Beta Battery**: Isotope containing scintillator and surrounding scintillator captures virtually all of the energy emitted by the beta emitter.

damage, their performance is far more tolerant of defects than that of semiconductor junctions. This allows the scintillator-based approach to use both higher energy isotopes and larger quantities of the isotopes. It is projected that this technology has the potential to produce a radioisotope battery with up to twice the efficiency of presently used systems.

This work was done by Noa M. Rensing, Michael R. Squillante, Timothy C. Tiernan,

William Higgins, and Urmila Shirwadkar of Radiation Monitoring Devices, Inc. for Glenn Research Center. Further information is contained in a TSP (see page 1). LEW-18871-1

Inquiries concerning rights for the commercial use of this invention should be addressed to NASA Glenn Research Center, Innovative Partnerships Office, Attn: Steven Fedor, Mail Stop 4-8, 21000 Brookpark Road, Cleveland, Ohio 44135. Refer to LEW-18871-1.

Magnetic Shield for Adiabatic Demagnetization Refrigerators (ADR)

NASA's Jet Propulsion Laboratory, Pasadena, California

A new method was developed for creating a less expensive shield for ADRs using 1018 carbon steel. This shield has been designed to have similar performance to the expensive vanadium permen-

dur shields, but the cost is 30 to 50% less. Also, these shields can be stocked in a variety of sizes, eliminating the need for special forgings, which also greatly reduces cost.

This work was done by Talso C. Chui and Nicolas E. Haddad of Caltech for NASA's Jet Propulsion Laboratory. For more information, contact iaoffice@jpl.nasa.gov. NPO-48732



CMOS-Compatible SOI MESFETS for Radiation-Hardened DC-to-DC Converters

Goddard Space Flight Center, Greenbelt, Maryland

A radiation-tolerant transistor switch has been developed that can operate between -196 and $+150$ °C for DC-to-DC power conversion applications. A prototype buck regulator component was demonstrated to be performing well after a total ionizing dose of 300 krad(Si). The prototype buck converters

showed good efficiencies at ultra-high switching speeds in the range of 1 to 10 MHz. Such high switching frequency will enable smaller, lighter buck converters to be developed as part of the next project. Switching regulators are widely used in commercial applications including portable consumer electronics.

This work was done by Trevor Thornton of Arizona State University and William Lepkowski and Seth Wilk of SJT Micropower for Goddard Space Flight Center. Further information is contained in a TSP (see page 1). GSC-16304-1

Silicon Heat Pipe Array

Applications include high-power electronic circuits or components such as microprocessors, diode lasers, and concentrated solar collectors.

NASA's Jet Propulsion Laboratory, Pasadena, California

Improved methods of heat dissipation are required for modern, high-power-density electronic systems. As increased functionality is progressively compacted into decreasing volumes, this need will be exacerbated. High-performance chip power is predicted to increase monotonically and rapidly with time. Systems utilizing these chips are currently reliant upon decades of old cooling technology.

Heat pipes offer a solution to this problem. Heat pipes are passive, self-contained, two-phase heat dissipation devices. Heat conducted into the device through a wick structure converts the working fluid into a vapor, which then releases the heat via condensation after being transported away from the heat source. Heat pipes have high thermal conductivities, are inexpensive, and have been utilized in previous space missions. However, the cylindrical geometry of commercial heat pipes is a poor fit to the planar geometries of micro-electronic assemblies, the copper that commercial heat pipes are typically constructed of is a poor CTE (coefficient of thermal expansion) match to the semiconductor die utilized in these assemblies, and the functionality and reliability of heat pipes in general is strongly dependent on the orientation of the assembly with respect to the gravity vector. What is needed is a planar, semiconductor-based heat pipe array that can be used for cooling of generic MCM (multichip module) assem-

blies that can also function in all orientations. Such a structure would not only have applications in the cooling of space electronics, but would have commercial applications as well (e.g. cooling of microprocessors and high-power laser diodes).

This technology is an improvement over existing heat pipe designs due to the finer porosity of the wick, which enhances capillary pumping pressure, resulting in greater effective thermal conductivity and performance in any orientation with respect to the gravity vector. In addition, it is constructed of silicon, and thus is better suited for the cooling of semiconductor devices.

The device consists of two silicon wafers, one of which has a mechanically drilled hole for a fill port. Each wafer is lithographically masked and etched to define a hermetic seal ring and the structural support elements. Each wafer then undergoes a mask-free cryo etch to define the black Si wick structure (the etch process developed results in an $\approx 3\times$ taller black Si structure than has been reported elsewhere). The wafers are then cleaned, thermally oxidized, and fusion-bonded together. Precision metering is then utilized to fill the device with the working fluid (e.g. water) through the fill port, which is then sealed off.

This device is able to absorb a large quantity of heat due to the phase change

of the working fluid, and transport the heat efficiently away from the source (i.e., it has a large effective thermal conductivity). Due to the small effective pore radius of the nanotextured surface, high capillary forces are exerted on the working fluid and the device is able to work in any orientation with respect to the gravity vector. In addition, due to the all silicon construction, the device is expansion-matched to the types of high-power die that would potentially be mounted to it.

The novel aspects of this assembly include:

- (1) Co-fabrication of the heat pipe structure and the wick. A black Si wick structure is utilized so that the housing of the heat pipe and the wick structure can be co-fabricated. This enables stress-free operation of the device over temperature, as the device is of homogenous material construction. Adhesion of the wick to the structure is not an issue, as the wick is etched from the structure itself, and is not grown or deposited.
- (2) Direct attachment or integration of heat-generating elements to the heat pipe. Fabrication of the heat pipe from Si allows stress-free, expansion-matched attachment of high-power semiconductor components or even the direct integration of such components. For example, high-power

semiconductor lasers could be solder-attached in modular fashion to the heat pipe, or could be made directly from the heat pipe structure itself for increased thermal efficiency. Another example would be the fabri-

cation of solar cells for use in concentrated solar collectors; co-fabrication of the heat pipe with the solar cells from the same silicon wafer would enable more efficient thermal management.

This work was done by Karl Y. Yee, Gani B. Ganapathi, Eric T. Sunada, Youngsam Bae, Jennifer R. Miller, and Daniel F. Berisford of Caltech for NASA's Jet Propulsion Laboratory. For more information, contact iaoffice@jpl.nasa.gov. NPO-47306

Adaptive Phase Delay Generator

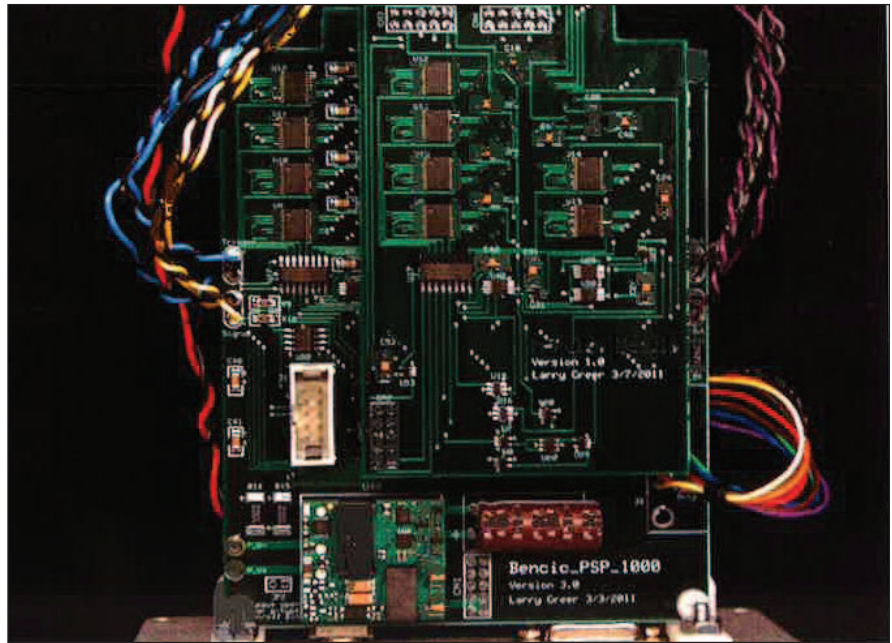
Test facilities that need to synchronize test equipment with rotating machinery could make use of this device.

John H. Glenn Research Center, Cleveland, Ohio

There are several experimental setups involving rotating machinery that require some form of synchronization. The adaptive phase delay generator (APDG) — the Bencic-1000 — is a flexible instrument that allows the user to generate pulses synchronized to the rising edge of a tachometer signal from any piece of rotating machinery. These synchronized pulses can vary by the delay angle, pulse width, number of pulses per period, number of skipped pulses, and total number of pulses. Due to the design of the pulse generator, any and all of these parameters can be changed independently, yielding an unparalleled level of versatility.

There are two user interfaces to the APDG. The first is a LabVIEW program that has the advantage of displaying all of the pulse parameters and input signal data within one neatly organized window on the PC monitor. Furthermore, the LabVIEW interface plots the rpm of the two input signal channels in real time. The second user interface is a handheld portable device that goes anywhere a computer is not accessible. It consists of a liquid-crystal display and keypad, which enable the user to control the unit by scrolling through a host of command menus and parameter listings.

The APDG combines all of the desired synchronization control into one unit. The experimenter can adjust the delay, pulse width, pulse count, number of skipped pulses, and produce a specified number of pulses per revolution. Each of these parameters can be changed independently, providing an unparalleled level of versatility when synchronizing



The construction of the **Adaptive Phase Delay Generator** allows for inclusion of multi-pulse functions by adding an expansion board to each channel.

hardware to a host of rotating machinery. The APDG allows experimenters to set up quickly and generate a host of synchronizing configurations using a simple user interface, which hopefully leads to faster results.

The heart of the Bencic-1000 is a reconfigurable pulse-generating state machine that cycles through three to four primary states, depending on the mode of operation. A second state machine tracks the period of the input signal by incorporating a latching synchronous 32-bit counter and a microcontroller. These hardware state machines make

use of high-speed CMOS technology, primarily from the HC family of parts, and have no problem operating with the 10-MHz master clock. The microcontroller is a 50-MHz 8051 derivative optimized to run at 50 MIPS.

This work was done by Lawrence Greer of Glenn Research Center. Further information is contained in a TSP (see page 1).

Inquiries concerning rights for the commercial use of this invention should be addressed to NASA Glenn Research Center, Innovative Partnerships Office, Attn: Steven Fedor, Mail Stop 4-8, 21000 Brookpark Road, Cleveland, Ohio 44135. Refer to LEW-18942-1.



High-Temperature, Lightweight, Self-Healing Ceramic Composites for Aircraft Engine Applications

Applications include the nuclear power generation industry and military ships.

John H. Glenn Research Center, Cleveland, Ohio

The use of reliable, high-temperature, lightweight materials in the manufacture of aircraft engines is expected to result in lower fossil and biofuel consumption, thereby leading to cost savings and lower carbon emissions due to air travel. Although nickel-based superalloy blades and vanes have been successfully used in aircraft engines for several decades, there has been an increased effort to develop high-temperature, lightweight, creep-resistant substitute materials under various NASA programs over the last two decades. As a result, there has been a great deal of interest in developing SiC/SiC ceramic matrix composites (CMCs) due to their higher damage tolerance compared to monolithic ceramics. Current-generation SiC/SiC ceramic matrix composites rely almost entirely on the SiC fibers to carry the load, owing to the premature cracking of the matrix during loading. Thus, the high-temperature usefulness of these CMCs falls well below their theoretical capabilities.

The objective of this work is to develop a new class of high-temperature, lightweight, self-healing, SiC fiber-reinforced, engineered matrix ceramic composites. Several engineered matrices

were designed to be thermally compatible with SiC. Several different tests were conducted on these matrices, which helped to down-select suitable compositions. Engineered matrix composites (EMCs) designed to match the coefficient of thermal expansion (CTE) of the SiC fiber were fabricated by slurry casting and melt infiltration techniques. The matrix composition was designed to convert any ingressed oxygen into low-viscosity oxides or silicates so they can flow into the cracks due to capillary action and seal them, thereby activating its self-healing properties.

The present concept uses the fundamental principles of physics and materials science to develop a new class of self-healing ceramic composites (SHCCs). Unlike current SiC/SiC CMC technology, the present concept develops SiC fiber-reinforced SiC-Si₃N₄-silicide matrix composites with a composition formulated to match the CTE of the fibers, and with an ability to get ingressed oxygen and self-heal cracks by filling them with low-viscosity oxides.

The present concept provides considerable flexibility in designing the composite matrix for a wide variety of high-

temperature applications. Depending on the composition, silicides deform plastically at high temperatures, unlike SiC and Si₃N₄. Thus, the matrix is likely to be compliant to the applied loading conditions at high temperatures rather than develop cracks. This important feature allows the matrix to carry some load before transferring to the reinforcing SiC fibers, extending the life of the composite. The ability of these matrices to self-heal fine cracks is also expected to increase composite life. For matrices containing (Cr,Mo)₃Si, the expected amount of free silicon after melt infiltration is expected to be low, which would allow composites made with this engineered matrix to be used in applications at or above 1,755 K.

This work was done by Sai V. Raj of Glenn Research Center, and Mrityunjay Singh and Ramkrishna Bhatt of the Ohio Aerospace Institute. Further information is contained in a TSP (see page 1).

Inquiries concerning rights for the commercial use of this invention should be addressed to NASA Glenn Research Center, Innovative Partnerships Office, Attn: Steven Fedor, Mail Stop 4-8, 21000 Brookpark Road, Cleveland, Ohio 44135. Refer to LEW-18964-1.

Treatment to Control Adhesion of Silicone-Based Elastomers

Ultraviolet radiation is used to control and decrease the level of adhesion.

John H. Glenn Research Center, Cleveland, Ohio

Seals are used to facilitate the joining of two items, usually temporarily. At some point in the future, it is expected that the items will need to be separated. This innovation enables control of the adhesive properties of silicone-based elastomers. The innovation may also be effective on elastomers other than the silicone-based ones. A technique has been discovered that decreases the level of adhesion of silicone-based elastomers to negligible levels. The new technique causes less dam-

age to the material compared to alternative adhesion mitigation techniques.

Silicone-based elastomers are the only class of “rubber-like” materials that currently meet NASA’s needs for various seal applications. However, silicone-based elastomers have natural inherent adhesive properties. This stickiness can be helpful, but it can frequently cause problems as well, such as when trying to get items apart.

In the past, seal adhesion was not always adequately addressed, and has

caused in-flight failures where seals were actually pulled from their grooves, preventing subsequent spacecraft docking until the seal was physically removed from the flange via an extravehicular activity (EVA). The primary method used in the past to lower elastomer seal adhesion has been the application of some type of lubricant or grease to the surface of the seal. A newer method uses ultraviolet (UV) radiation — a mixture of UV wavelengths in the range of near ultravi-

olet (NUV) and vacuum ultraviolet (VUV) wavelengths. UV radiation also causes damage to the seal, with different wavelengths causing different levels of damage.

Low-wavelength VUV radiation attenuates rapidly; it is absorbed quickly and does not penetrate deeply into solids or gases. VUV is absorbed by air, thus does not reach the surface of Earth. Seals exposed to near-VUV radiation achieve the desired level of adhesion reduction without raising the seal leakage level. The radiation likely breaks weaker atomic bonds on long polymer molecules near the sur-

face, which can then cross-link with other molecules, thereby absorbing the weaker bonds and preventing adhesive bonds.

The novel feature of the innovation is that it uses near-VUV wavelength radiation to control and decrease the level of adhesion of silicone-based elastomers without significantly damaging the elastomer. It is expected that the innovation can be implemented using handheld radiation sources, thereby enabling the technique to be used on odd-shaped and very large parts.

The innovation has the potential to use off-the-shelf radiation sources in air,

thus circumventing the need for a vacuum chamber. Exposures could be done, for example, using a radiation “oven” through which a conveyor belt passes.

This work was done by Henry C. de Groh III, Bernadette J. Puleo, and Deborah L. Waters of Glenn Research Center. Further information is contained in a TSP (see page 1).

Inquiries concerning rights for the commercial use of this invention should be addressed to NASA Glenn Research Center, Innovative Partnerships Office, Attn: Steven Fedor, Mail Stop 4-8, 21000 Brookpark Road, Cleveland, Ohio 44135. Refer to LEW-18948-1.

High-Temperature Adhesives for Thermally Stable Aero-Assist Technologies

These adhesives feature high thermal conductivity and increased thermal decomposition temperature.

Marshall Space Flight Center, Alabama

Aero-assist technologies are used to control the velocity of exploration vehicles (EVs) when entering Earth or other planetary atmospheres. Since entry of EVs in planetary atmospheres results in significant heating, thermally stable aero-assist technologies are required to avoid the high heating rates while maintaining low mass. Polymer adhesives are used in aero-assist structures because of the need for high flexibility and good bonding between layers of polymer films or fabrics. However, current polymer adhesives cannot withstand temperatures above 400 °C.

This innovation utilizes nanotechnology capabilities to address this need, leading to the development of high-temperature adhesives that exhibit high thermal conductivity in addition to increased thermal decomposition temperature. Enhanced thermal conductivity will help to dissipate heat quickly and effectively to avoid temperature rising to harmful levels. This, together with increased thermal decomposition temperature, will enable the adhesives to sustain transient high-temperature conditions.

A first principle analysis showed that enhancing the thermal conductivity of

the adhesive can have a beneficial impact on the high-temperature stability of aeroshells and inflatable structures. Silicones and polyimides are used as high-temperature adhesives, and prior efforts have been made to incorporate thermally conductive ceramic powders such as aluminum oxide and boron nitride into silicone formulations to increase thermal conductivity. These high loading levels of ceramic particles present several problems. Viscosity rises, necessitating the use of a solvent, which then needs to be removed at a later stage. Adhesive and mechanical properties deteriorate. A way to decrease the additive loading level while achieving the desired thermal performance was needed.

For conventional composite structures, a three-dimensional percolative network is required to achieve significant performance enhancement, which typically results in a high-volume loading of particles. In contrast, advances were made in creating a new paradigm in non-three-dimensional percolative composites. The emphasis is on nanoparticulate composites, but the concept applies equally well to all particulate composites

(i.e., both nanoscale and microscale). As a result, the desired thermal properties can be obtained at relatively low loading levels of nanoparticles, without the detrimental effect on processing and other properties, such as mechanical strength and bonding.

The thermal conductivity of silicone material can be significantly enhanced by adding high-aspect-ratio nanoparticles at relatively low levels. For example, the thermal conductivity is drastically increased by a factor of 3.7 when 10 wt % of high-aspect-ratio nanoparticles is added to a commercial silicone adhesive. In addition, it was shown that there is a synergistic effect when spherical nanoparticles and high-aspect-ratio particles are present. An array of samples that had unique nanoparticle characteristics and nanocomposite morphology was fabricated, and a set of characterization protocols was developed.

This work was done by Kenneth Eberts and Runqing Ou of NEI Corp. for Marshall Space Flight Center. For more information, contact Sammy Nabors, MSFC Commercialization Assistance Lead, at sammy.a.nabors@nasa.gov. Refer to MFS-32899-1.



Rockballer Sample Acquisition Tool

This tool also has application in the medical industry in the removal of tissue samples or tumors from the body.

NASA's Jet Propulsion Laboratory, Pasadena, California

It would be desirable to acquire rock and/or ice samples that extend below the surface of the parent rock or ice in extraterrestrial environments such as the Moon, Mars, comets, and asteroids. Such samples would allow measurements to be made further back into the geologic history of the rock, providing critical insight into the history of the local environment and the solar system. Such samples could also be necessary for sample return mission architectures that would acquire samples from extraterrestrial environments for return to Earth for more detailed scientific investigation.

Conventional methods for the acquisition of rock or ice use devices similar to augers, drills, core drills, or hole saws to cut a cylindrical sample from the parent rock. These cylindrical sample acquisition methods suffer from two fundamental problems. First, cylindrical methods tend to leave an uncut circular root that attaches the base of the sample to the parent rock so separating the sample may require significant force. Second, cylindrical methods also do not guarantee that a sample will remain within the cutting tool after cutting. It is possible to add mechanisms to cylindrical mechanisms that may increase the thickness of the cutting tool, which increases the amount of rock that must be displaced ("cuttings") in order for the tool to cut into the rock. The increased volume of cuttings does not increase the amount of sample acquired, but it does increase the time and electrical energy required to acquire a sample, and thus this solution is undesirable.

The Rockballer circumvents the issues of both sample separation and sample retention by eliminating the cylindrical cutting methods in favor of a new spherical cutting method. This spherical cutting method is achieved through the use of two cutting "jaws" that are essentially formed by cutting a thin hemispherical shell into two symmetric parts. The jaws are slowly closed around the sample as the entire Rock-

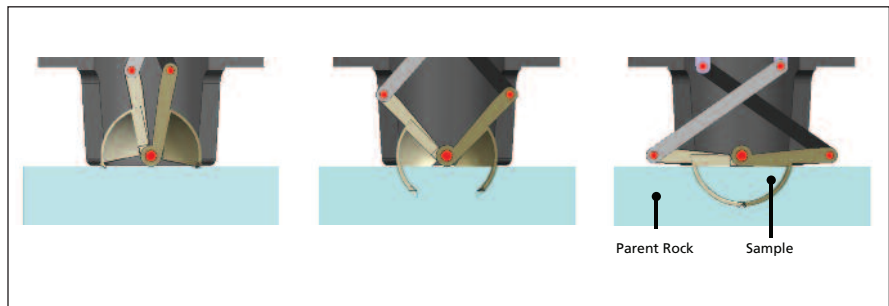


Figure 1. The sequence shows a cutaway view of how the Rockballer cuts and retains a sample as the jaws close. The rapid rotation about the vertical tool axis is not shown.

baller rotates about an axis normal to the parent rock. As these jaws close, they simultaneously dig deeper into the parent rock and surround the sample, thus achieving sample acquisition and retention with a single process. When acquisition of the sample is complete, the Rockballer is withdrawn with the sample secured within the closed jaws. The Rockballer can then be repositioned, for example, near a science instrument or sample transfer mechanism, and the jaws can be opened to release the sample in a controlled and predictable fashion.

The resulting samples are hemispherical or nearly hemispherical and as a result, the aspect ratio (sample depth relative to sample radius) is essentially fixed. This fixed sample aspect ratio may be considered a drawback of the Rockballer, as samples with a higher aspect ratio (more depth, less width) may be considered more scientifically valuable because these samples would allow for a broader inspection of the geological record. This aspect ratio issue could be ameliorated if the Rockballer is paired with a Rock Abrasion Tool (RAT) similar to those used on the Mars Exploration Rovers. The RAT would be used to first grind into the surface of the parent rock, after which the Rockballer would extract a sample from deeper in the rock than would have been possible without first using the RAT.

The Rockballer has the added advantage of being able to also function as a



Figure 2. Photograph of Soapstone Sample (left) cut from parent rock (right) by the Rockballer prototype; the sample is 14.8 mm deep and has a mass of 26 grams.

scoop for acquiring granular dust, regolith, soil, or small rocks. Consequently, the Rockballer is both a mini-coring tool and scoop.

The prototype Rockballer successfully cut and retained rock samples from both soapstone and alabaster. The prototype Rockballer was designed to cut rock samples roughly 1.5 cm deep with a mass of roughly 25 g; these dimensions were selected based on a hypothetical Mars Sample Return mission concept; however, the Rockballer can be designed to produce samples of any size. Soapstone and alabaster were selected because these rocks are relatively soft and readily available; however, the Rockballer can be designed to cut samples from any type of rock or ice.

This work was done by Louis R. Giersch and Brant T. Cook of Caltech for NASA's Jet Propulsion Laboratory. For more information, contact iaoffice@jpl.nasa.gov. NPO-47715

⚙️ Rock Gripper for Sampling, Mobility, Anchoring, and Manipulation

This spine/claw-based technology has applications in military robots that need to climb natural rock surfaces or caves for reconnaissance purposes, or for revealing buried explosive devices.

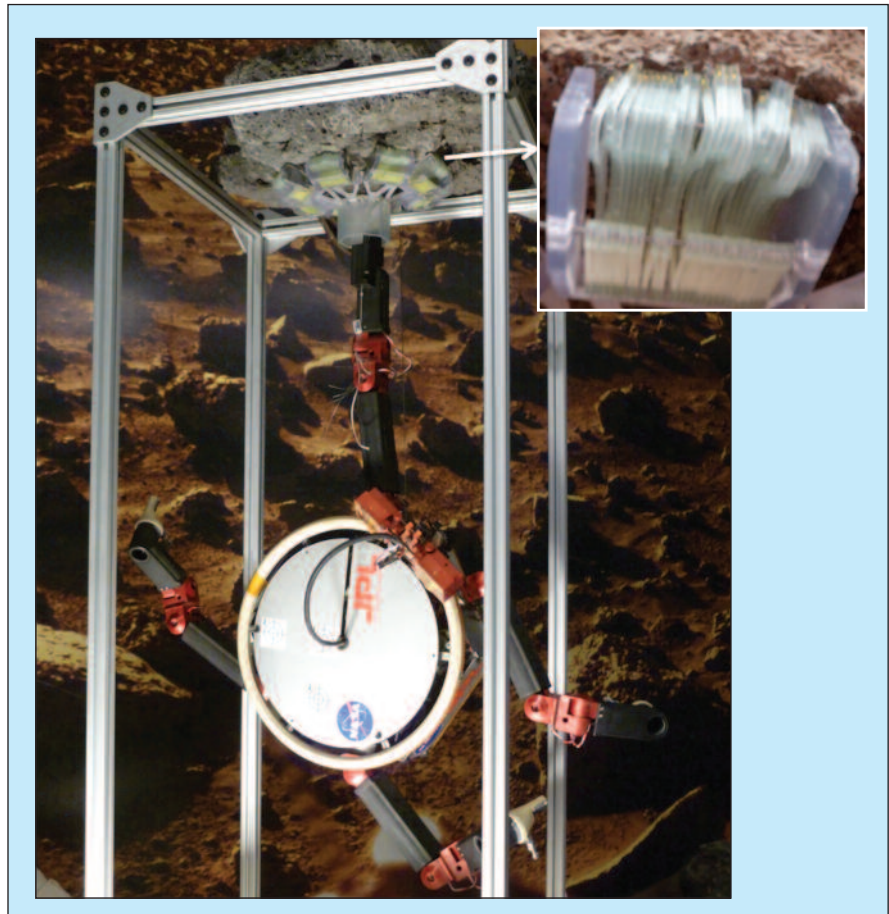
NASA's Jet Propulsion Laboratory, Pasadena, California

A new gripper mechanism can be used as an end effector for a long arm that reaches out from a nearby spacecraft for a touch-and-go type of mission. The gripper would stabilize the arm and allow samples to be collected and in situ science to be done from a fixed platform. In the long term, this style of gripper could even be used as handholds for astronauts trying to move about on/near small asteroids. The prototype developed has demonstrated a 120 N gripping force, and improvements continue to be made.

The gripping mechanism is useful not only for low-gravity bodies, but for steep surfaces on Mars and the Moon. The clawed toes used in the gripping mechanism were originally developed for climbing rough surfaces like brick and tree bark, but have been expanded in this work to attach to natural rock surfaces. Using an opposed gripping mechanism provides the maximum stability for this type of system, where reliability is critical. In a similar application on Earth, these grippers allow the exploration of cliff faces, cave ceilings, glacial ice features, and underwater reefs and sea floor. This gripper can also be used as an under-actuated robotic hand for grasping, manipulating, and probing rocks on the surface of a planetary body.

The gripper uses several hundred microspine toes that each have an independent suspension system, allowing them to conform to a rock surface and find a suitable asperity to grip. Each microspine toe consists of a steel hook embedded in a rigid frame with a compliant suspension system. By arraying tens or hundreds of these microspine toes, large loads can be supported and shared among many attachment points. The hooks can attach to both convex and concave asperities like pits, protrusions, or even sloped rock faces.

This design is scalable to loads as small as a few Newtons and as large as 1,000 N or more, as demonstrated by previous work in climbing configurations. To create an omni-directional anchor, eight rows of 30 toes each were attached to an octagonal center housing.



The Lemur IIb Robot hangs its weight off of a vesicular basalt rock using a prototype gripper.

Each row of toes is held in place by a leg that acts as a lever with the pivot point at the outer rim of the housing. Several lever dimensions were tried empirically to determine a good ratio of lengths. The center of the housing is hollow, providing an accessible location for mounting the anchor to the leg of a robot or placing a sampling tool like a coring drill.

Microspine technology is extended with the development of mechanisms that create internal forces at the foot-scale for arrays of microspine toes in opposed configurations. Locating internal forces at the foot-scale decouples the limbs, allowing each leg to attach/detach independently. This reduces the

control demand on the robot and lowers cost and weight.

This work was done by Aaron Parness of Caltech for NASA's Jet Propulsion Laboratory. For more information, contact iaoffice@jpl.nasa.gov.

In accordance with Public Law 96-517, the contractor has elected to retain title to this invention. Inquiries concerning rights for its commercial use should be addressed to:

*Innovative Technology Assets Management
JPL*

*Mail Stop 202-233
4800 Oak Grove Drive
Pasadena, CA 91109-8099*

E-mail: iaoffice@jpl.nasa.gov

Refer to NPO-47990, volume and number of this NASA Tech Briefs issue, and the page number.



Advanced Magnetic Materials Methods and Numerical Models for Fluidization in Microgravity and Hypogravity

Solid wastes can be gasified for the recovery of valuable resources.

Lyndon B. Johnson Space Center, Houston, Texas

To support long-duration manned missions in space such as a permanent lunar base, Mars transit, or Mars Surface Mission, improved methods for the treatment of solid wastes, particularly methods that recover valuable resources, are needed. The ability to operate under microgravity and hypogravity conditions is essential to meet this objective. The utilization of magnetic forces to manipulate granular magnetic media has provided the means to treat solid wastes under variable gravity conditions by filtration using a consolidated magnetic media bed followed by thermal processing of the solid wastes in a fluidized bed reactor.

Non-uniform magnetic fields will produce a magnetic field gradient in a bed of magnetically susceptible media toward the distributor plate of a fluidized bed reactor. A correctly oriented magnetic field gradient will generate a downward direct force on magnetic media that can substitute for gravitational force in microgravity, or which may augment low levels of gravity, such as on the Moon or Mars. This approach is termed Gradient Magnetically Assisted Fluidization (G-MAFB), in which the magnitude of

the force on the fluidized media depends upon the intensity of the magnetic field (H), the intensity of the field gradient (dH/dz), and the magnetic susceptibility of the media. Fluidized beds based on the G-MAFB process can operate in any gravitational environment by tuning the magnetic field appropriately.

Magnetic materials and methods have been developed that enable G-MAFB operation under variable gravity conditions. Ferromagnetic, porous cobalt particles were prepared for use as filtration media. Magnetic body forces can be used to consolidate granular ferromagnetic media into a bed forming a depth filter for the separation of particulate matter from a gas or liquid stream. During filtration, such a depth filter can be expanded using these magnetic methods to create additional void space into which waste particles can be confined, thereby increasing filtration capacity. At the end of the filtration event, the bed can be fluidized to release a concentrated slug of particulate matter for processing elsewhere or can be employed as a fluidized gasification reactor. When used as a filter, G-MAFB methods result

in a regenerable particle filter, since entrained particles are released during fluidization, and after re-consolidation of the magnetic media, the bed is available for another filtration cycle.

G-MAFB methods combined with ferromagnetic catalyst media provide the basis for highly efficient, fluidized bed, catalytic reactors in which solid wastes can be gasified for the recovery of valuable resources. As such, fluidization of ferromagnetic catalyst particles at high temperature offers higher rates of mass transfer than are achievable in other reactors, whether fluidized or not, since the degree of bed expansion can be controlled using the magnetic force to augment gravity regardless of flow conditions. G-MAFB methods may also be used in a wide variety of other processes in which fluidization is employed for a variety of unit operations.

This work was done by James Atwater, Richard Wheeler, Jr., and James Akse of UMPQUA Research Company; and Goran Jovanovic and Brian Reed of Oregon State University for Johnson Space Center. Further information is contained in a TSP (see page 1). MSC-24245-1

Data Transfer for Multiple Sensor Networks Over a Broad Temperature Range

Unique codes may be generated to distinguish among the signals from sensors coming in via a common medium.

John H. Glenn Research Center, Cleveland, Ohio

At extreme temperatures, cryogenic and over 300 °C, few electronic components are available to support intelligent data transfer over a common, linear combining medium. This innovation allows many sensors to operate on the same wire bus (or on the same airwaves or optical channel: any linearly combining medium), transmitting simultaneously, but individually re-

coverable at a node in a cooler part of the test area.

This innovation has been demonstrated using room-temperature silicon microcircuits as proxy. The microcircuits have analog functionality comparable to componentry designed using silicon carbide. Given a common, linearly combining medium, multiple sending units may transmit information simultaneously. A

listening node, using various techniques, can pick out the signal from a single sender, if it has unique qualities, e.g. a “voice.” The problem being solved is commonly referred to as the cocktail party problem. The human brain uses the cocktail party effect when it is able to recognize and follow a single conversation in a party full of talkers and other noise sources.

High-temperature sensors have been used in silicon carbide electronic oscillator circuits. The frequency of the oscillator changes as a function of the changes in the sensed parameter, such as pressure. This change is analogous to changes in the pitch of a person's voice.

The output of this oscillator and many others may be superimposed onto a single medium. This medium may be the power lines supplying current to the sensors, a third wire dedicated to data transmission, the airwaves through radio transmission, an optical medium, etc. However, with nothing to distin-

guish the identities of each source — that is, the source separation — this system is useless.

Using digital electronic functions, unique codes or patterns are created and used to modulate the output of the sensor. By using a dividend of the oscillator frequency to generate the code, a constant a priori number of oscillator cycles will define each bit. At the receiver, a detected frequency will be correlated with stored code patterns to find a match. If detected and verified as coming from a known sender, a frequency will be disassociated from noise and

from other transmitting sensors in that it has a unique modulation pattern or "voice." The length of the detected code, or instantaneously, the frequency detected, is the measure, and intelligent data transfer has been accomplished.

This work was done by Michael Krasowski of Glenn Research Center. Further information is contained in a TSP (see page 1).

Inquiries concerning rights for the commercial use of this invention should be addressed to NASA Glenn Research Center, Innovative Partnerships Office, Attn: Steven Fedor, Mail Stop 4-8, 21000 Brookpark Road, Cleveland, Ohio 44135. Refer to LEW-18910-1.

Using Combustion Synthesis to Reinforce Berms and Other Regolith Structures

New structures will require a minimum of maintenance and upkeep.

Lyndon B. Johnson Space Center, Houston, Texas

The Moonraker Excavator and other tools under development for use on the Moon, Mars, and asteroids will be employed to construct a number of civil engineering projects and to mine the soil. Mounds of loose soil will be subject to the local transport mechanisms plus artificial mechanisms such as blast effects from landers and erosion from surface vehicles. Some of these structures will require some permanence, with a minimum of maintenance and upkeep.

Combustion Synthesis (CS) is a family of processes and techniques whereby chemistry is used to transform materials, often creating flame in a hard vacuum. CS can be used to stabilize civil engineering works such as berms, habitat shielding, ramps, pads, roadways, and the like. The method is to unroll thin sheets of CS fabric between layers of regolith and then fire the fabric, creating a

continuous sheet of crusty material to be interposed among layers of loose regolith. The combination of low-energy processes, ISRU (in situ resource utilization) excavator, and CS fabrics, seems compelling as a general method for establishing structures of some permanence and utility, especially in the role of robotic missions as precursors to manned exploration and settlement.

In robotic precursory missions, excavator/mobility ensembles mine the Lunar surface, erect constructions of soil, and dispense sheets of CS fabrics that are covered with layers of soil, fired, and then again covered with layers of soil, iterating until the desired dimensions and forms are achieved. At the base of each berm, for example, is a shallow trench lined with CS fabric, fired and filled, mounded, and then covered and fired, iteratively to provide a footing against lateral shear. A larger

trench is host to a habitat module, back-filled, covered with fabric, covered with soil, and fired.

Covering the applied CS fabric with layers of soil before firing allows the resulting matrix to incorporate soil both above and below the fabric ply into the fused layer, developing a very irregular surface which, like sandpaper, can provide an anchor for loose soil. CS fabrics employ a coarse fiberglass weave that persists as reinforcement for the fired material. The fiberglass softens at a temperature that exceeds the combustion temperature by factors of two to three, and withstands the installation process.

This type of structure should be more resistant to rocket blast effects from Lunar landers.

This work was done by Gary Rodriguez of sysRAND Corporation for Johnson Space Center. Further information is contained in a TSP (see page 1). MSC-24411-1

Visible-Infrared Hyperspectral Image Projector

Goddard Space Flight Center, Greenbelt, Maryland

The VisIR HIP generates spatially-spectrally complex scenes. The generated scenes simulate real-world targets viewed by various remote sensing instruments. The VisIR HIP consists of two subsystems: a spectral engine and a spa-

tial engine. The spectral engine generates spectrally complex uniform illumination that spans the wavelength range between 380 nm and 1,600 nm. The spatial engine generates two-dimensional gray-scale scenes. When combined, the

two engines are capable of producing two-dimensional scenes with a unique spectrum at each pixel. The VisIR HIP can be used to calibrate any spectrally sensitive remote-sensing instrument. Tests were conducted on the Wide-field

Imaging Interferometer Testbed at NASA's Goddard Space Flight Center.

The device is a variation of the calibrated hyperspectral image projector developed by the National Institute of Standards and Technology in Gaithersburg, MD. It uses Gooch & Housego Visible and Infrared OL490 Agile Light

Sources to generate arbitrary spectra. The two light sources are coupled to a digital light processing (DLP™) digital mirror device (DMD) that serves as the spatial engine. Scenes are displayed on the DMD synchronously with desired spectrum. Scene/spectrum combinations are displayed in rapid succession,

over time intervals that are short compared to the integration time of the system under test.

This work was done by Matthew Bolcar of Goddard Space Flight Center. Further information is contained in a TSP (see page 1). GSC-16422-1

Three-Axis Attitude Estimation With a High-Bandwidth Angular Rate Sensor

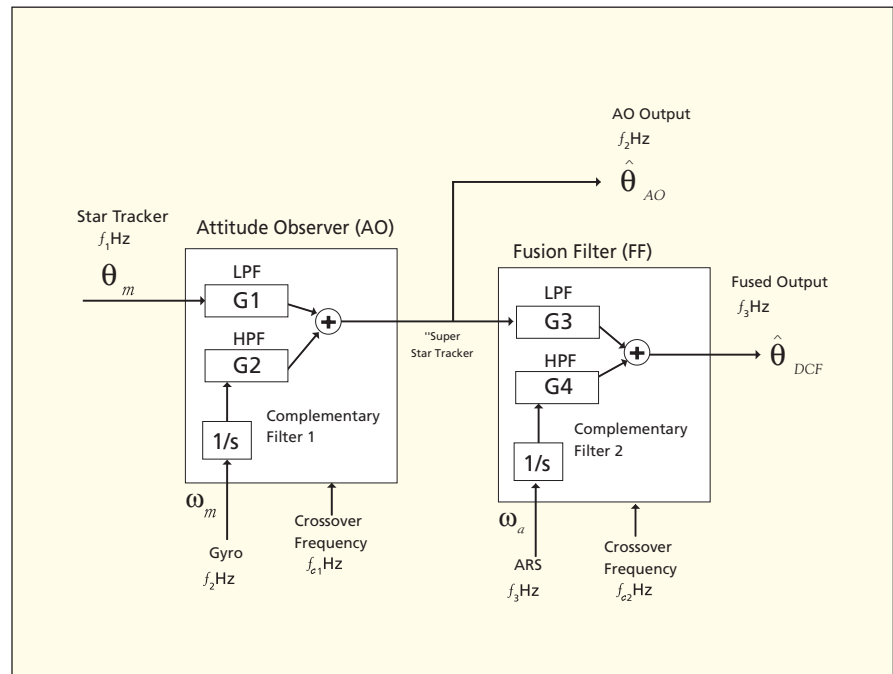
Commercial applications include pointing of cameras on space telescopes, spacecraft instrument payloads, moving vehicles, and surveillance from airborne platforms.

NASA's Jet Propulsion Laboratory, Pasadena, California

A continuing challenge for modern instrument pointing control systems is to meet the increasingly stringent pointing performance requirements imposed by emerging advanced scientific, defense, and civilian payloads. Instruments such as adaptive optics telescopes, space interferometers, and optical communications make unprecedented demands on precision pointing capabilities. A cost-effective method was developed for increasing the pointing performance for this class of NASA applications.

The solution was to develop an attitude estimator that fuses star tracker and gyro measurements with a high-bandwidth angular rotation sensor (ARS). An ARS is a rate sensor whose bandwidth extends well beyond that of the gyro, typically up to 1,000 Hz or higher. The most promising ARS sensor technology is based on a magnetohydrodynamic concept, and has recently become available commercially. The key idea is that the sensor fusion of the star tracker, gyro, and ARS provides a high-bandwidth attitude estimate suitable for supporting pointing control with a fast-steering mirror or other type of tip/tilt correction for increased performance. The ARS is relatively inexpensive and can be bolted directly next to the gyro and star tracker on the spacecraft bus.

The high-bandwidth attitude estimator fuses an ARS sensor with a standard three-axis suite comprised of a gyro and star tracker. The estimation architecture is based on a dual-complementary filter (DCF) structure. The DCF takes a frequency-weighted combination of the sensors such that each sensor is most heavily weighted in a frequency region where it has the lowest noise.



Dual Complementary Filter (DCF) architecture blends ARS with star tracker and gyro measurements to produce an accurate high-bandwidth attitude estimate. (Note: LPF and HPF are low-pass and high-pass filters, respectively.)

An important property of the DCF is that it avoids the need to model disturbance torques in the filter mechanization. This is important because the disturbance torques are generally not known in applications. This property represents an advantage over the prior art because it overcomes a weakness of the Kalman filter that arises when fusing more than one rate measurement.

An additional advantage over prior art is that, computationally, the DCF requires significantly fewer real-time calculations than a Kalman filter formulation. There are essentially two reasons

for this: the DCF state is not augmented with angular rate, and measurement updates occur at the slower gyro rate instead of the faster ARS sampling rate.

Finally, the DCF has a simple and compelling architecture. The DCF is exactly equivalent to flying two identical attitude observers, one at low rate and one at high rate. These attitude observers are exactly of the form currently flown on typical three-axis spacecraft.

This work was done by David S. Bayard and Joseph J. Green of Caltech for NASA's Jet Propulsion Laboratory. Further information is contained in a TSP (see page 1). NPO-48171



Change_Detection.m

The Change_Detection.m MATLAB tool detects changes in an image by comparing the image to a background estimation. The change detection software is a MATLAB function designed to work on either a single image or a sequence of images, and computes changes with respect to a background image by one of four techniques:

1. Frame-to-frame change detection — the change detection image represents the difference between two frames.
2. Rolling median change detection — the change detection image represents the difference between an image and a median background estimation taken over a subset of the total frames presented to the function.
3. Rolling mean change detection — the change detection image represents the difference between an image and a mean background estimation taken over a subset of the total frames presented to the function.
4. Rolling mode change detection — the change detection image represents the difference between an image and a mode background estimation taken over a subset of the total frames presented to the function.

The software is an improvement on other scripting techniques by functionalizing the code with an INPUT/OUTPUT structure format that may work either at the command line or in conjunction with a separate graphic user interface function. The function also allows periodic background estimations instead of background estimations on a per-frame basis.

All computation is done on grayscale imagery, so color or multispectral images will be first converted to grayscale. Differences from the background that exceed a preset threshold are reported as changes in the form of a returned binary mask.

The algorithm can work in single-frame or multi-frame mode. In single-frame mode, only one image is being investigated for changes relative to a background. In multi-frame mode, a sequence of images is being investigated for changes relative to the background.

After the image changes are detected, the image is then converted into a bi-

nary representation of the change detection image by setting a threshold. The threshold is given as multiples of a standard deviation of the values in the difference image (the difference between the image and the background). The binary change detection mask is then multiplied by the original image in the sequence to obtain the values of the pixels that have changed. The outputted mask is the same size as the inputted frame, but now only the pixels that have changed are non-zero.

This work was done by David M. Palacios and Steven J. Lewis of Caltech for NASA's Jet Propulsion Laboratory. Further information is contained in a TSP (see page 1).

This software is available for commercial licensing. Please contact Daniel Broderick of the California Institute of Technology at danielb@caltech.edu. Refer to NPO-47671.

AGATE: Adversarial Game Analysis for Tactical Evaluation

AGATE generates a set of ranked strategies that enables an autonomous vehicle to track/trail another vehicle that is trying to break the contact using evasive tactics. The software is efficient (can be run on a laptop), scales well with environmental complexity, and is suitable for use onboard an autonomous vehicle. The software will run in near-real-time (2 Hz) on most commercial laptops. Existing software is usually run offline in a planning mode, and is not used to control an unmanned vehicle actively.

JPL has developed a system for AGATE that uses adversarial game theory (AGT) methods (in particular, leader-follower and pursuit-evasion) to enable an autonomous vehicle (AV) to maintain tracking/trailing operations on a target that is employing evasive tactics. The AV trailing, tracking, and reacquisition operations are characterized by imperfect information, and are an example of a non-zero sum game (a positive payoff for the AV is not necessarily an equal loss for the target being tracked and, potentially, additional adversarial boats). Previously, JPL successfully applied the Nash equilibrium method for onboard control of an autonomous ground vehicle (AGV) traveling over hazardous terrain.

This work was done by Terrance L. Huntsberger of Caltech for NASA's Jet Propulsion

Laboratory. Further information is contained in a TSP (see page 1).

This software is available for commercial licensing. Please contact Daniel Broderick of the California Institute of Technology at danielb@caltech.edu. Refer to NPO-48697.

Ionospheric Simulation System for Satellite Observations and Global Assimilative Modeling Experiments (ISOGAME)

ISOGAME is designed and developed to assess quantitatively the impact of new observation systems on the capability of imaging and modeling the ionosphere. With ISOGAME, one can perform observation system simulation experiments (OSSEs). A typical OSSE using ISOGAME would involve: (1) simulating various ionospheric conditions on global scales; (2) simulating ionospheric measurements made from a constellation of low-Earth-orbiters (LEOs), particularly Global Navigation Satellite System (GNSS) radio occultation data, and from ground-based global GNSS networks; (3) conducting ionospheric data assimilation experiments with the Global Assimilative Ionospheric Model (GAIM); and (4) analyzing modeling results with visualization tools. ISOGAME can provide quantitative assessment of the accuracy of assimilative modeling with the interested observation system. Other observation systems besides those based on GNSS are also possible to analyze.

The system is composed of a suite of software that combines the GAIM, including a 4D first-principles ionospheric model and data assimilation modules, an Internal Reference Ionosphere (IRI) model that has been developed by international ionospheric research communities, observation simulator, visualization software, and orbit design, simulation, and optimization software.

The core GAIM model used in ISOGAME is based on the GAIM++ code (written in C++) that includes a new high-fidelity geomagnetic field representation (multi-dipole). New visualization tools and analysis algorithms for the OSSEs are now part of ISOGAME.

This work was done by Xiaoqing Pi, Anthony J. Mannucci, Olga P. Verkhoglyadova, Philip Stephens, Brian D. Wilson, Vardan Akopian, Attila Komjathy, and Byron A. Iijima of Caltech

for NASA's Jet Propulsion Laboratory. For more information, contact iaoffice@jpl.nasa.gov.

This software is available for commercial licensing. Please contact Daniel Broderick of the California Institute of Technology at danielb@caltech.edu. Refer to NPO-47779.

An Extensible, User-Modifiable Framework for Planning Activities

This software provides a development framework that allows planning activities for the Mars Science Laboratory rover to be altered at any time, based on changes of the Activity Dictionary. The Activity Dictionary contains the definition of all activities that can be carried out by a particular asset (robotic or human). These definitions (and combinations of these definitions) are used by mission planners to give a daily plan of what a mission should do. During the development and course of the mission, the Activity Dictionary and actions that are going to be carried out will often be changed. Previously, such changes would require a change to the software and redeployment. Now, the Activity Dictionary authors are able to customize activity definitions, parameters, and resource usage without requiring redeployment.

This software provides developers and end users the ability to modify the behavior of automatically generated activities using a script. This allows changes to the software behavior without incurring the burden of redeployment. This software is currently being used for the Mars Science Laboratory, and is in the process of being

integrated into the LADEE (Lunar Atmosphere and Dust Environment Explorer) mission, as well as the International Space Station.

This work was done by Joseph C. Joshing, Lucy Abramyan, Megan C. Mickelson, Michael N. Wallick, James A. Kurien, Thomas M. Crockett, and Mark W. Powell of Caltech; Guy Pyrzak of Ames Research Center; and Arash Aghevoli of Stinger Ghaffarian Technologies for NASA's Jet Propulsion Laboratory. For more information, contact iaoffice@jpl.nasa.gov.

This software is available for commercial licensing. Please contact Daniel Broderick of the California Institute of Technology at danielb@caltech.edu. Refer to NPO-48308.

Mission Operations Center (MOC) - Precipitation Processing System (PPS) Interface Software System (MPISS)

MPISS is an automatic file transfer system that implements a combination of standard and mission-unique transfer protocols required by the Global Precipitation Measurement Mission (GPM) Precipitation Processing System (PPS) to control the flow of data between the MOC and the PPS. The primary features of MPISS are file transfers (both with and without PPS specific protocols), logging of file transfer and system events to local files and a standard messaging bus, short term storage of data files to facilitate retransmissions, and generation of file transfer accounting reports. The system includes a graphical

user interface (GUI) to control the system, allow manual operations, and to display events in real time. The PPS specific protocols are an enhanced version of those that were developed for the Tropical Rainfall Measuring Mission (TRMM).

All file transfers between the MOC and the PPS use the SSH File Transfer Protocol (SFTP). For reports and data files generated within the MOC, no additional protocols are used when transferring files to the PPS. For observatory data files, an additional handshaking protocol of data notices and data receipts is used. MPISS generates and sends to the PPS data notices containing data start and stop times along with a checksum for the file for each observatory data file transmitted. MPISS retrieves the PPS generated data receipts that indicate the success or failure of the PPS to ingest the data file and/or notice. MPISS retransmits the appropriate files as indicated in the receipt when required. MPISS also automatically retrieves files from the PPS.

The unique feature of this software is the use of both standard and PPS specific protocols in parallel. The advantage of this capability is that it supports users that require the PPS protocol as well as those that do not require it. The system is highly configurable to accommodate the needs of future users.

This work was done by Jeffrey Ferrara, William Calk, William Atwell, and Tina Tsui of Goddard Space Flight Center. Further information is contained in a TSP (see page 1). GSC-16238-1



Automated 3D Damaged Cavity Model Builder for Lower Surface Acreage Tile on Orbiter

The principles may be applicable to commercial space vehicles.

Lyndon B. Johnson Space Center, Houston, Texas

The 3D Automated Thermal Tool for Damaged Acreage Tile Math Model builder was developed to perform quickly and accurately 3D thermal analyses on damaged lower surface acreage tiles and structures beneath the damaged locations on a Space Shuttle Orbiter. The 3D model builder created both TRASYS geometric math models (GMMs) and SINDA thermal math models (TMMs) to simulate an idealized damaged cavity in the damaged tile(s). The GMMs are processed in TRASYS to generate radiation conductors between the surfaces in the cavity. The radiation conductors are inserted into the TMMs, which are processed in SINDA to generate temperature histories for all of the nodes on each layer of the TMM.

The invention allows a thermal analyst to create quickly and accurately a 3D model of a damaged lower surface tile on the orbiter. The 3D model builder can generate a GMM and the corresponding TMM in one or two minutes, with the damaged cavity included in the tile material. A separate program creates a configuration file, which would take a

couple of minutes to edit. This configuration file is read by the model builder program to determine the location of the damage, the correct tile type, tile thickness, structure thickness, and SIP thickness of the damage, so that the model builder program can build an accurate model at the specified location. Once the models are built, they are processed by the TRASYS and SINDA.

Before the existence of this automated process, a thermal analyst would manually build a 2D or 3D damaged tile model or modify an existing model by hand. However, existing models that are available only cover a portion of the lower surface of the orbiter, and the 2D models cannot be used to calculate realistic thermal gradients in the structure layer. If an existing model for the damaged location is available, the thermal analyst would make manual edits to the model, removing or modifying the nodes in the model to simulate the damaged cavity. The model may require additional modifications if the simulated location was built with the incorrect tile thickness, tile type, or structure thick-

ness. In addition, if the cavity in the model required heating augmentation factors, the factors would have to be manually added to the model. These manual processes can be very time consuming and prone to editing errors.

The automation of the damaged cavity model, GMM, and TMM allows the thermal analyst to build thousands of models with varying cavity dimensions at various locations on the bottom of the orbiter. The results from all the model runs were merged into a set of damage tolerance maps that allows trained personnel to quickly screen a damaged cavity found in the on-orbit photos to see if the damage site required additional analysis. Although the system is specific to the Space Shuttle Orbiter in its current configuration, it is able to be re-programmed to support any commercial space vehicle that uses tiles as part of its external surface.

This work was done by Shannon Belknap and Michael Zhang of The Boeing Company for Johnson Space Center. For further information, contact the JSC Innovation Partnerships Office at (281) 483-3809. MSC-25177-1

Mixed Linear/Square-Root Encoded Single-Slope Ramp Provides Low-Noise ADC With High Linearity for Focal Plane Arrays

This technique is applicable to all scientific imagers and could be used by commercial camera vendors.

NASA's Jet Propulsion Laboratory, Pasadena, California

Single-slope analog-to-digital converters (ADCs) are particularly useful for on-chip digitization in focal plane arrays (FPAs) because of their inherent monotonicity, relative simplicity, and efficiency for column-parallel applications, but they are comparatively slow. Square-root encoding can allow the number of code values to be reduced without loss of

signal-to-noise ratio (SNR) by keeping the quantization noise just below the signal shot noise. This encoding can be implemented directly by using a quadratic ramp. The reduction in the number of code values can substantially increase the quantization speed. However, in an FPA, the fixed pattern noise (FPN) limits the use of small quantization steps at

low signal levels. If the zero-point is adjusted so that the lowest column is on-scale, the other columns, including those at the center of the distribution, will be pushed up the ramp where the quantization noise is higher.

Additionally, the finite frequency response of the ramp buffer amplifier and the comparator distort the shape of

the ramp, so that the effective ramp value at the time the comparator trips differs from the intended value, resulting in errors. Allowing increased settling time decreases the quantization speed, while increasing the bandwidth increases the noise.

The FPN problem is solved by breaking the ramp into two portions, with some fraction of the available code values allocated to a linear ramp and the remainder to a quadratic ramp. To avoid large transients, both the value and the slope of the linear and quadratic portions should be equal where they join. The span of the linear portion must cover the minimum offset, but not necessarily the maximum, since the fraction of the pixels above the upper limit will still be correctly quantized, albeit with increased quantization noise. The required linear span, maximum signal and ratio of quantization noise to shot noise at high signal, along with the continuity requirement, determines the number of code values that must be allocated to each portion.

The distortion problem is solved by using a lookup table to convert captured code values back to signal levels. The values in this table will be similar to the intended ramp value, but with a correction for the finite bandwidth effects.

Continuous-time comparators are used, and their bandwidth is set below the step rate, which smoothes the ramp and reduces the noise. No settling time is needed, as would be the case for clocked comparators, but the low bandwidth enhances the distortion of the non-linear portion. This is corrected by use of a return lookup table, which differs from the one used to generate the ramp. The return lookup table is obtained by calibrating against a stepped precision DC reference. This results in a residual non-linearity well below the quantization noise. This method can also compensate for differential non-linearity (DNL) in the DAC used to generate the ramp.

The use of a ramp with a combination of linear and quadratic portions for a single-slope ADC is novel. The number of steps is minimized by keeping the step

size just below the photon shot noise. This in turn maximizes the speed of the conversion. High resolution is maintained by keeping small quantization steps at low signals, and noise is minimized by allowing the lowest analog bandwidth, all without increasing the quantization noise. A calibrated return lookup table allows the system to maintain excellent linearity.

This work was done by Chris J. Wrigley, Bruce R. Hancock, Kenneth W. Newton, and Thomas J. Cunningham of Caltech for NASA's Jet Propulsion Laboratory. Further information is contained in a TSP (see page 1).

In accordance with Public Law 96-517, the contractor has elected to retain title to this invention. Inquiries concerning rights for its commercial use should be addressed to:

*Innovative Technology Assets Management
JPL*

Mail Stop 202-233

4800 Oak Grove Drive

Pasadena, CA 91109-8099

E-mail: iaoffice@jpl.nasa.gov

Refer to NPO-47836, volume and number of this NASA Tech Briefs issue, and the page number.

RUSHMAPS: Real-time Uploadable Spherical Harmonic Moment Analysis for Particle Spectrometers

High-performing hybrid systems embed unprecedented amounts of onboard processing power.

Goddard Space Flight Center, Greenbelt, Maryland

RUSHMAPS is a new onboard data reduction scheme that gives real-time access to key science parameters (e.g. moments) of a class of heliophysics science and/or solar system exploration investigation that includes plasma particle spectrometers (PPS), but requires moments reporting (density, bulk-velocity, temperature, pressure, etc.) of higher-level quality, and tolerates a low-pass (variable quality) spectral representation of the corresponding particle velocity distributions, such that telemetry use is minimized. The proposed methodology trades access to the full-resolution velocity distribution data, saving on telemetry, for real-time access to both the moments and an adjustable-quality (increasing quality increases volume) spectral representation of distribution functions.

Traditional onboard data storage and downlink bandwidth constraints severely limit PPS system functionality and drive cost, which, as a consequence, drives a

limited data collection and lower angular energy and time resolution. This prototypical system exploit, using high-performance processing technology at GSFC (Goddard Space Flight Center), uses a SpaceCube and/or Maestro-type platform for processing. These processing platforms are currently being used on the International Space Station as a technology demonstration, and work is currently ongoing in a new onboard computation system for the Earth Science missions, but they have never been implemented in heliospheric science or solar system exploration missions.

Preliminary analysis confirms that the targeted processor platforms possess the processing resources required for real-time application of these algorithms to the spectrometer data. SpaceCube platforms demonstrate that the target architecture possesses the sort of compact, low-mass/power, radiation-tolerant characteristics needed for flight. These high-performing hybrid systems embed

unprecedented amounts of onboard processing power in the CPU (central processing unit), FPGAs (field programmable gate arrays), and DSP (digital signal processing) elements. The fundamental computational algorithm deconstructs 3D velocity distributions in terms of spherical harmonic spectral coefficients (which are analogous to a Fourier sine-cosine decomposition), but uses instead spherical harmonics Legendre polynomial orthogonal functions as a basis for the expansion, portraying each 2D angular distribution at every energy or, geometrically, spherical speed-shell swept by the particle spectrometer. Optionally, these spherical harmonic spectral coefficients may be telemetered to the ground. These will provide a smoothed description of the velocity distribution function whose quality will depend on the number of coefficients determined.

Successfully implemented on the GSFC-developed processor, the capabil-

ity to integrate the proposed methodology with both heritage and anticipated future plasma particle spectrometer designs is demonstrated (with sufficiently detailed design analysis to advance

TRL) to show specific science relevancy with future HSD (Heliophysics Science Division) solar-interplanetary, planetary missions, sounding rockets and/or CubeSat missions.

This work was done by Adolfo Figueroa-Vinas of Goddard Space Flight Center. Further information is contained in a TSP (see page 1). GSC-16455-1

➤ Powered Descent Guidance With General Thrust-Pointing Constraints

NASA's Jet Propulsion Laboratory, Pasadena, California

The Powered Descent Guidance (PDG) algorithm and software for generating Mars pinpoint or precision landing guidance profiles has been enhanced to incorporate thrust-pointing constraints. Pointing constraints would typically be needed for onboard sensor and navigation systems that have specific field-of-view requirements to generate valid ground proximity and terrain-relative state measurements.

The original PDG algorithm was designed to enforce both control and state constraints, including maximum and minimum thrust bounds, avoidance of the ground or descent within a glide slope cone, and maximum speed limits. The thrust-bound and thrust-pointing constraints within PDG are non-convex,

which in general requires nonlinear optimization methods to generate solutions. The short duration of Mars powered descent requires guaranteed PDG convergence to a solution within a finite time; however, nonlinear optimization methods have no guarantees of convergence to the global optimal or convergence within finite computation time.

A lossless convexification developed for the original PDG algorithm relaxed the non-convex thrust bound constraints. This relaxation was theoretically proven to provide valid and optimal solutions for the original, non-convex problem within a convex framework. As with the thrust bound constraint, a relaxation of the thrust-pointing constraint also provides a lossless convexifi-

cation that ensures the enhanced relaxed PDG algorithm remains convex and retains validity for the original non-convex problem. The enhanced PDG algorithm provides guidance profiles for pinpoint and precision landing that minimize fuel usage, minimize landing error to the target, and ensure satisfaction of all position and control constraints, including thrust bounds and now thrust-pointing constraints.

This work was done by John M. Carson III, Behcet Acikmese, and Lars Blackmore of Caltech for NASA's Jet Propulsion Laboratory. For more information, contact iaoffice@jpl.nasa.gov.

This software is available for commercial licensing. Please contact Daniel Broderick of the California Institute of Technology at danielb@caltech.edu. Refer to NPO-47853.

➤ X-Ray Detection and Processing Models for Spacecraft Navigation and Timing

Combining different pulsar measurements provides accurate overall navigation for deep space vehicles.

Goddard Space Flight Center, Greenbelt, Maryland

The current primary method of deep-space navigation is the NASA Deep Space Network (DSN). High-performance navigation is achieved using Delta Differential One-Way Range techniques that utilize simultaneous observations from multiple DSN sites, and incorporate observations of quasars near the line-of-sight to a spacecraft in order to improve the range and angle measurement accuracies.

Over the past four decades, x-ray astronomers have identified a number of x-ray pulsars with pulsed emissions having stabilities comparable to atomic clocks. The x-ray pulsar-based navigation and time determination (XNAV) system uses phase measurements from these sources to establish autonomously the position of

the detector, and thus the spacecraft, relative to a known reference frame, much as the Global Positioning System (GPS) uses phase measurements from radio signals from several satellites to establish the position of the user relative to an Earth-centered fixed frame of reference. While a GPS receiver uses an antenna to detect the radio signals, XNAV uses a detector array to capture the individual x-ray photons from the x-ray pulsars. The navigation solution relies on detailed x-ray source models, signal processing, navigation and timing algorithms, and analytical tools that form the basis of an autonomous XNAV system.

Through previous XNAV development efforts, some techniques have

been established to utilize a pulsar pulse time-of-arrival (TOA) measurement to correct a position estimate. One well-studied approach, based upon Kalman filter methods, optimally adjusts a dynamic orbit propagation solution based upon the offset in measured and predicted pulse TOA. In this delta position estimator scheme, previously estimated values of spacecraft position and velocity are utilized from an onboard orbit propagator. Using these estimated values, the detected arrival times at the spacecraft of pulses from a pulsar are compared to the predicted arrival times defined by the pulsar's pulse timing model. A discrepancy provides an estimate of the spacecraft position offset,

since an error in position will relate to the measured time offset of a pulse along the line of sight to the pulsar. XNAV researchers have been developing additional enhanced approaches to process the photon TOAs to arrive at an estimate of spacecraft position, including those using maximum-likelihood estimation, digital phase locked loops,

and “single photon processing” schemes that utilize all available time data associated with each photon. Using pulsars from separate, non-coplanar locations provides range and range-rate measurements in each pulsar’s direction. Combining these different pulsar measurements solves for offsets in position and velocity in three dimensions, and pro-

vides accurate overall navigation for deep space vehicles.

This work was done by Suneel Sheikh of ASTER Labs, Inc., John Hanson of CrossTrac Engineering, Inc., and Paul Graven of Cateni, Inc. and Microcosm, Inc. for Goddard Space Flight Center. Further information is contained in a TSP (see page 1). GSC-16116-1



Extreme Ionizing-Radiation-Resistant Bacterium

***Deinococcus phoenicis* sp. nov. can be used as an indicator for sterilization processes in food, aerospace, medical, and pharmaceutical applications.**

NASA's Jet Propulsion Laboratory, Pasadena, CA

There is a growing concern that desiccation and extreme radiation-resistant, non-spore-forming microorganisms associated with spacecraft surfaces can withstand space environmental conditions and subsequent proliferation on another solar body. Such forward contamination would jeopardize future life detection or sample return technologies. The prime focus of NASA's planetary protection efforts is the development of strategies for inactivating resistance-bearing microorganisms. Eradication techniques can be designed to target resistance-conferring microbial populations by first identifying and understanding their physiologic and biochemical capabilities that confers its elevated tolerance (as is being studied in *Deinococcus phoenicis*, as a result of this description). Furthermore, hospitals, food, and government agencies frequently use biological indicators to ensure the efficacy of a wide range of radiation-based sterilization processes. Due to their resistance to a variety of perturbations, the non-spore forming *D. phoenicis* may be a more appropriate biological indicator than those currently in use.

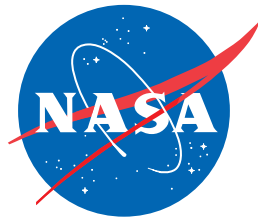
The high flux of cosmic rays during space travel and onto the unshielded surface of Mars poses a significant hazard to the survival of microbial life. Thus, radiation-resistant microorgan-

isms are of particular concern that can survive extreme radiation, desiccation, and low temperatures experienced during space travel. Spore-forming bacteria, a common inhabitant of spacecraft assembly facilities, are known to tolerate these extreme conditions. Since the Viking era, spores have been utilized to assess the degree and level of microbiological contamination on spacecraft and their associated spacecraft assembly facilities. Members of the non-sporeforming bacterial community such as *Deinococcus radiodurans* can survive acute exposures to ionizing radiation (5 kGy), ultraviolet light (1 kJ/m²), and desiccation (years). These resistive phenotypes of *Deinococcus* enhance the potential for transfer, and subsequent proliferation, on another solar body such as Mars and Europa. These organisms are more likely to escape planetary protection assays, which only take into account presence of spores. Hence, presences of extreme radiation-resistant *Deinococcus* in the cleanroom facility where spacecraft are assembled pose a serious risk for integrity of life-detection missions.

The microorganism described herein was isolated from the surfaces of the cleanroom facility in which the Phoenix Lander was assembled. The isolated bacterial strain was subjected to a compre-

hensive polyphasic analysis to characterize its taxonomic position. This bacterium exhibits very low 16S rRNA similarity with any other environmental isolate reported to date. Both phenotypic and phylogenetic analyses clearly indicate that this isolate belongs to the genus *Deinococcus* and represents a novel species. The name *Deinococcus phoenicis* was proposed after the Phoenix spacecraft, which was undergoing assembly, testing, and launch operations in the spacecraft assembly facility at the time of isolation. *D. phoenicis* cells exhibited higher resistance to ionizing radiation (cobalt-60; 14 kGy) than the cells of the *D. radiodurans* (5 kGy). Thus, it is in the best interest of NASA to thoroughly characterize this organism, which will further assess in determining the potential for forward contamination. Upon the completion of genetic and physiological characteristics of *D. phoenicis*, it will be added to a planetary protection database to be able to further model and predict the probability of forward contamination.

This work was done by Parag A. Vaishampayan and Kasthuri J. Venkateswaran of Caltech, and Petra Schwendner of Institute of Aerospace Medicine, German Aerospace Center (DLR), Germany for NASA's Jet Propulsion Laboratory. For more information, contact iaoffice@jpl.nasa.gov. NPO-48008



National Aeronautics and
Space Administration